Aerosol Catalysis: the Influence of Particle Structure on the Catalytic Activity of Platinum-Nanoparticle Agglomerates

by **Martin Seipenbusch***, **Joachim Binnig**, **Michael Heim**, **Alfred P. Weber**, and **Gerhard Kasper**

Institut für Mechanische Verfahrenstechnik und Mechanik, Universität Karlsruhe (TH), Kaiserstrasse 12, D-76128 Karlsruhe

Dedicated to Professor *André M. Braun* on the occasion of his 60th birthday

The structure of nanoparticle agglomerates can have substantial influence on their catalytic activity, as shown here for the oxidation of hydrogen on platinum nanoparticles. The structure of aerosol agglomerates was varied by thermally induced rearrangement of the so-called primary particles, which were *ca.* 5 nm in size. In this way, the fraction of outer surface, which is directly accessible for molecules from the gas phase, was varied from a very open agglomerate structure to massive spheres. A Monte-Carlo (MC) simulation of the surface phenomena was carried out parallel to the experiments, taking into account models for reactions including adsorption, surface diffusion, and desorption. Comparison of the experimental results with these MC simulations indicated that, for gas-borne nanoparticles, special features appear. For instance, the time scales of experiments and simulations are not identical. This discrepancy can be explained by altered adsorption kinetics on the nanoparticles compared to the kinetics on bulk surfaces, which was introduced into the MC simulation. The assumption of a lower sticking probability for molecules impinging from the gas phase as proposed before in other investigations leads to a shift in the time scale of the MC simulation as well as an increased sticking probability for O-atoms relative to the H-atom sticking probability. In addition, the surface-normalized catalytic activity, given by the turn-over rate (*TOR*), is higher for 5-nm than for 50-nm particles. Thus, the combination of experiments and simulation may be a useful tool to gain deeper insight into the influence of the properties of catalyst particles on the catalytic activity, whereby the simulation covers the subsecond time range, which is hardly accessible by experimentation.

1. Introduction. – In heterogeneous catalysis, metallic nanoparticles are widely used for the favorable ratio of surface area to catalyst mass to reduce costs, especially for precious metals. For experiments at normal pressures, these particles are conventionally supported by a porous material to maintain the degree of catalyst dispersion under reaction conditions. If the catalytic activity of the nanoparticles themselves is to be determined, several problems occur with this arrangement. The pores of the support material limit the rates of diffusion-controlled reactions by mass transfer of educts to the catalyst particles and of products into the gas phase. Electronic effects that occur between support material and catalyst can hardly be quantified. The contribution of the support material to the reaction can also happen in a more direct way. Spillover of activated species [1] from the catalyst onto the surface of the support material can occur, extending the surface available for the catalytic reaction partly to the 'inert' metallic nanoparticles, so that specific phenomena, *e.g.* surface state of the catalyst or particle morphology, cannot be observed apart from these effects.

Experiments in ultrahigh vacuum on particles supported on single-crystal wafers can give information on the reaction kinetics, even for single catalyst particles [2]. The transferability of the results obtained from these experiments to real catalytic processes at elevated pressures under reaction conditions, though, is questionable.

An experimental method that avoids the problems mentioned above for the characterization of the catalytic activity of nanoparticles and operates under technical reaction conditions in respect of temperature and pressure is offered by aerosol catalysis, introduced in 1996 by *Glikin et al.* [3]. The catalyst is suspended directly in the reaction gas as an aerosol, whereby pore diffusion and contact of the catalyst to another material is avoided. Particle morphology and surface condition of the particles can be adjusted, and the effect on the catalytic activity can be monitored [4]. On- and off-line aerosol characterization methods can be utilized to determine the particle properties and alterations induced by the reaction.

The reaction chosen for the determination of the catalytic activity of Pt-nanoparticles is the oxidation of H_2. Since its discovery by *Döbereiner* in 1823, this reaction has attracted abundant attention from a great number of researchers. The H_2/O_2 reaction is very well-suited for the development of a basic understanding of catalytic oxidation reactions since heterogenous reactions of H_2 and O_2 occur in most catalytic oxidations. The reaction was found to take place even at temperatures as low as 120 K [5]. To study morphological effects on the reaction, the low reaction temperatures are very favorable since elevated temperatures lead to alterations in the agglomerate and in the surface structure of the catalyst particles. The absence of permanent surface species with the oxidation of H_2 on Pt-surfaces again prevents time-dependent evolution of the surface state and catalytic activity due to self-poisoning effects.

The aim of the presented work is the determination of the influence of the particle structure on the apparent catalytic activity of gas-borne Pt nanoparticles for the test reaction. Aerosol catalysis experiments are compared with a Monte-Carlo (MC) simulation of adsorption, diffusion, and reaction processes at the particle surface.

2. Theory and Model of the Surface Phenomena. – *Reaction Mechanism: Elementary Steps.* Mass transport of the reaction gases H_2 and O_2 onto the particle surface, the first step for a reaction, can be modeled by the kinetic theory of gases. The rate of molecule impingement on the particle surface per area r_{imp} is given by *Eqn. 1*, with the partial pressure of the educt gas p_i, the molecule mass m_i, the *Boltzmann* constant k, and the temperature T.

$$r_{imp} = \frac{P_i}{\sqrt{2 \cdot \pi \cdot m_i \cdot k \cdot T}} \tag{1}$$

The surface area available for direct impingement of gas molecules from the gas phase can be determined from the mean diameter of first collisions with gas molecules, which is basically equivalent to the mobility-equivalent diameter obtainable from differential mobility analyzer (DMA) measurements [6]. This means that the inner surface of the agglomerates is inaccessible for direct adsorption from the gas phase and can be reached only by surface diffusion of the adsorbed species.

Adsorption of molecular H_2 is very unlikely to occur [7]. The molecule, though, dissociates with a very low activation energy on Pt surfaces (2 kJ mol^{-1} on Pt (111) [8]) and adsorbs atomically.

The sticking coefficient S for H-atoms on Pt-surfaces, defined as the ratio of the rate of adsorption to the collision rate i, varies strongly with the surface structure. Values for the initial sticking coefficient $S(0)$ for the uncovered surface at 300 K range from 0.02 to

0.2 for Pt(111) and from 0.005–0.4 for polycrystalline surfaces [8][9]. The broad variation of the values determined experimentally on extended surfaces shows a high sensitivity of the adsorption process towards inpurities [10][11] and crystallographic alterations, *e.g.* due to heating. The kinetics of adsorption, described by the coverage (θ)-dependent sticking coefficient, can be modeled by a simple *Langmuir* mechanism (see *Eqn. 2*), where the exponent μ describes the order of the adsorption process with respect to the concentration of uncovered adsorption sites on the Pt-surface and, for most reactions, equals the number of surface sites needed for adsorption. Therefore, for molecular adsorption, $\mu = 1$, and for dissociative adsorption, $\mu = 2$. Since the surface diffusion of the H-atoms is very fast, H_2 adsorption, although dissociative, is commonly modeled by a first-order *Langmuir* mechanism with $\mu = 1$ [12]. The evaluation of our MC model though suggested the use of a more complex relation between the sticking coefficient and the surface coverage. The model introduced by *Kisliuk* [13] takes the existence of a precursor state into account and is used commonly for adsorption kinetics more complex than a simple *Langmuir* mechanism [14]. In our MC simulation, a dissociative *Kisliuk* mechanism is utilized. The first step in this model is the physisorption of a nondissociated molecule to a weakly bonded precursor state. The model discriminates between the intrinsic precursor state, when the molecule is physisorbed over a covered adsorption site. From the initial state, the molecule has several options: it can desorb again, chemisorb onto the surface, or move to the next adsorption site. For every option, the model attributes a probability of its incidence. The blocking of surface sites by chemisorbed molecules is taken into account customarily by the introduction of the coverage θ. The dependence of the sticking coefficient on Θ is described by *Eqn. 3*, where the constant C is the ratio of the probabilities of the adsorption or desorption processes with p'_{des} being the probability for the desorption of the intrinsic and p''_{des} the probability for the desorption of the extrinsic precursor molecule.

$$S(\Theta) = S(0) \cdot (1 - \theta)^{\mu} \tag{2}$$

$$S(\theta) = \frac{S(0) \cdot (1 - \theta)}{1 + \dfrac{\theta}{(1 - \theta)} \cdot C + \dfrac{\theta^2}{(1 - \theta)} \cdot S(0)} \quad \text{with} \quad C = \frac{p''_{\mathrm{des}} - p'_{\mathrm{des}}}{p'_{\mathrm{ads}} + p'_{\mathrm{des}}} \tag{3}$$

The desorption of the chemisorbed H_{ads} is recombinative for temperatures lower than 1000 K. Literature values for the desorption energy range from 63–88 kJ mol^{-1} [8]. The desorption energy decreases with increasing surface coverage; the basis for this phenomenon is still obscure [8][15]. For the MC simulation, the activation energy for desorption E_a^{des} of H_{ads} was modeled as suggested by *Deutschmann* [8], who found *Eqn. 4* to best fit the results of experiments and simulation.

$$E_a^{\mathrm{des}} = (67.4 - 6 \cdot \theta_{H_{ads}})\,\mathrm{kJ\,mol^{-1}} \tag{4}$$

The adsorption of O_2 on the Pt-surface is dissociative as well in the temperature range of interest [16]. The dissociation occurs *via* a short-lived precursor state of adsorbed molecular O_2. The desorption energy of the $O_{2,ads}$ molecule though is higher

than the activation energy for the dissociation reaction [17]. At 300 K, experimentally determined values for $S(0)$ range from 0.04 to 0.25 [8][9] for Pt(111) and from 0.05 to 0.4 for polycrystalline Pt-surfaces. The modeling in our MC model of the adsorption of O_2 on Pt is, as commonly done [8][18][19], carried out with a second-order *Langmuir* mechanism. Desorption of the chemisorbed O_{ads} is neglected in the model.

The reaction product H_2O_{ads} is adsorbed molecularly on Pt, and it desorbs very fast at temperatures exceeding 200 K [8]. In our model, the assumption is made that water desorbs directly after formation.

The OH radical, a reaction intermediate, can desorb and readsorb on the surface. Desorption energies were found to range from 192 to 256 kJ mol^{-1} [8]. For the activation energy of adsorption, a value of 15 kJ mol^{-1} was determined [20].

Surface diffusion is of crucial importance for the overall reaction kinetics. The velocity of diffusion is determined principally by the bonding energy between adsorbed atom and adsorption site, surface coverage (by the blocking of adsorption sites and attractive or repulsive interactions between adsorbed species), and temperature. Measurements of the surface diffusion resulted in an activation energy of 68 ± 5 meV and a pre-exponential factor of $(1.1 \pm 0.5) \cdot 10^{-3}$ cm^2 s^{-1} for adsorbed H-atoms in a temperature range $140 \leq T \leq 250$ K and a surface coverage in the range 0.05 ML $\leq \theta \leq$ 0.66 ML [21]. For the surface diffusion of oxygen, an activation energy of 430 meV and a pre-exponential factor of $5 \cdot 10^{-3}$ cm^2 s^{-1} were determined for temperatures around 200 K [22]. The *Arrhenius* form of the kinetics of surface diffusion of the H- and O-atoms is of importance. The reaction of OH_{ads} with H_{ads} to H_2O occurs very fast because of the high mobility of the H_{ads} on the surface so that the surface diffusion of OH radical can be neglected.

The formation of water follows a *Langmuir-Hinshelwood* path [8][23]. In a first step, the adsorbed atoms react to form OH_{ads} (*Eqn. 5*). Together with another H_{ads}, the OH_{ads} forms H_2O_{ads} (*Eqn. 6*). Parallel to this reaction, the combination of two OH_{ads} to form O_{ads} and H_2O_{ads} occurs (*Eqn. 7*). The adsorbed water molecules desorb rapidly. For the MC simulation, a spontaneous reaction of surface species is assumed once they are adsorbed to neighboring surface sites. This simplification is justified, since the aim of this work is not the quantitative description of the reaction mechanism but the determination of the qualitative effect of agglomerate structure on the surface phenomena resulting in an overall catalytic activity. *Eqn. 8* describes an autocatalytic process as suggested by *Völkening et al.* below the desorption temperature of water (170 K) and under ultrahigh vacuum [16]. Although aerosol catalysis operates at atmospheric pressure, we do not expect water to be adsorbed on the surface long enough to make autocatalysis possible since the surface temperature far exceeded the desorption temperature [24].

$$H_{ads} + O_{ads} \rightarrow OH_{ads} \tag{5}$$

$$H_{ads} + OH_{ads} \rightarrow H_2O_{ads} \rightarrow H_2O \tag{6}$$

$$OH_{ads} + OH_{ads} \rightarrow O_{ads} + H_2O_{ads} \rightarrow O_{ads} + H_2O \tag{7}$$

$$H_2O_{ads} + O_{ads} \rightarrow 2\ OH_{ads} \tag{8}$$

3. Modeling of the Surface and Agglomerate Structure. – For the MC simulation, the surface was modeled homogeneously, assuming that every surface site is equally active for adsorption, desorption, and reaction. For the surface of a spherical particle, where every surface site is available for adsorption from the gas phase, a square lattice of 100×100 sites was modeled with a periodic boundary condition between the borders to eliminate edge effects.

The agglomerate (see *Fig. 1*) was modeled as a two-dimensional lattice of 432×432 representing 12×12 primary particles, each consisting of 35×35 surface sites (including borders between the primary particles of 12 sites), corresponding to a 5-nm Pt-particle (*Fig. 2*). The contact area between the primary particles was 7 sites wide, as estimated applying the *Johnson-Kendall-Roberts* (JKR) theory on 5-nm Pt-particles [25]. The coordination number rises from 1 for the outermost particle to 4 approaching the center of the agglomerate. The average coordination number was 2.5, in agreement with other investigations [26]. Only the primary particles in the white area of *Fig. 2* are accessible to molecules diffusing from the gas phase. The internal surface area, represented by the primary particles in the gray area, can be accessed only *via* surface diffusion. The ratio K of the outer surface to the total surface of the model agglomerate was varied by assigning more or less primary particles to the white zone (*Fig. 2*) where molecules from the gas phase can impinge.

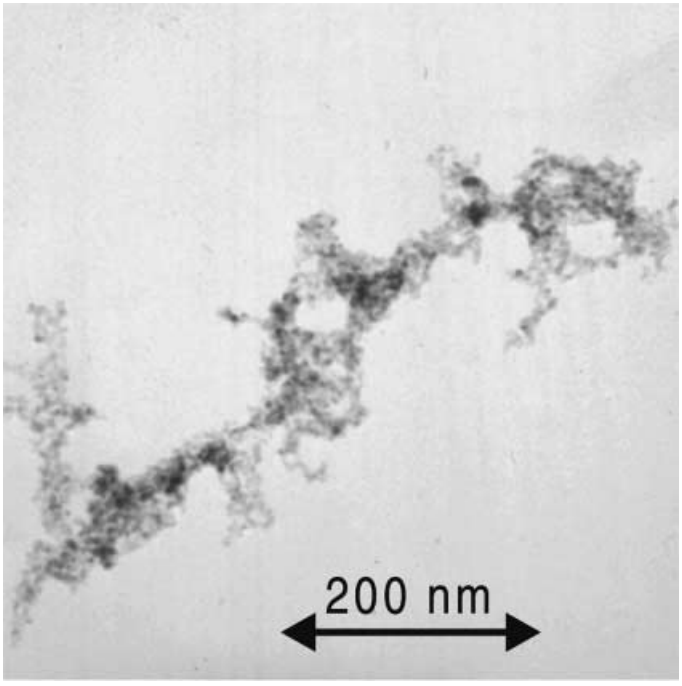

Fig. 1. *Transmission electron spectroscopy* (TEM) *micrograph of Pt-agglomerate produced in the spark discharge generator*

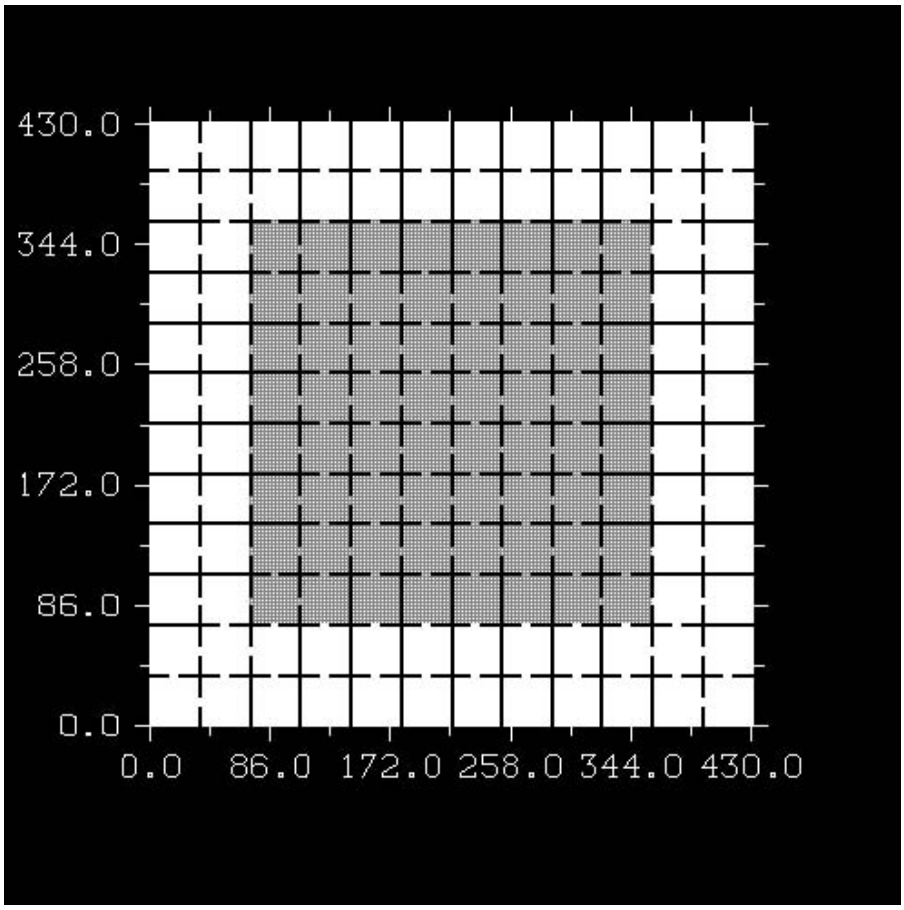

Fig. 2. *Model array of the agglomerate surface for the MC simulation.* The white area is accessible to diffusing gas molecules for impingement, the gray area represents the inner surface accessible only *via* surface diffusion.

4. Monte-Carlo Model of the Surface Phenomena. – Our model was developed as a dynamic MC model in which the behavior of the system over time is simulated. The mechanisms relevant for the time step are the rates of impingement of the educt molecules, the rate of desorption of H_2, and the rates of surface diffusion for the surface species O and H. All of these rates, except for the molecule impingement, are dependent on the surface coverage and thus vary with time. The time step is calculated according to *Eqn. 5*.

$$\tau = \frac{1}{r_{\mathrm{imp,H_2}} + r_{\mathrm{imp,O_2}} + r_{\mathrm{des,H_2}} + r_{\mathrm{diff,H_{ads}}} + r_{\mathrm{diff,O_{ads}}}} \tag{5}$$

At every time step, which is of the order of 10^{-17} – 10^{-16} s and is itself a function of time, one of the three mechanisms takes place with the probability of its incidence. If the step leads to a change in the surface coverage, the rates are calculated for the new condition.

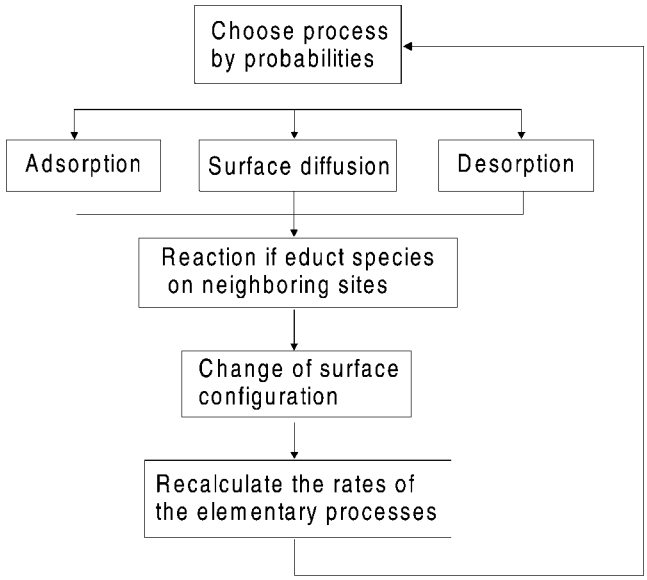

Fig. 3. *Flow chart of the Monte-Carlo simulation: single cycle of one time increment with elementary steps*

An instantaneous chemical reaction occurs when two educt molecules of one of the possible reactions are situated at neighboring adsorption sites. The time increment τ is added to the total run time. *Fig. 3* shows a flow chart for a single cycle of the MC simulation with the elementary steps.

An optimization for a high H_{ads} surface coverage θ_H is implemented for the case where no O_{ads} or OH_{ads} is present at the surface. When this occurs, a certain number of time steps (432^3 for the agglomerate equivalent to 432 surface movements per adsorbed species at $\theta = 1$) is carried out to reach a good distribution of H on the surface before the rates of surface diffusion are set to zero until an O_2 molecule adsorbs or a H_2 molecule desorbs. The time increment is increased when surface diffusion is set to zero, thus leaving the temporal behavior of the entire process unaffected but saving machine time for the calculations.

An integral turn-over rate (*TOR*) is calculated from the number of product molecules generated over the total run time of the simulation, the total number of surface sites in the lattice, and the total run time.

5. Experimental. – To utilize aerosol catalysis for the characterization of the catalytic activity of agglomerates of Pt-nanoparticles in the aerosol state, an aerosol is produced in a spark-discharge generator [27], consisting of two Pt-electrodes in parallel with a capacitor charged by a high-vacuum source. When the breakdown voltage is reached, the capacitor discharges by spark between the electrodes, evaporating a small amount of electrode material into the inert carrier gas. Due to the rapid cooling, homogeneous condensation sets in, leaving a very high number concentration of Pt-particles. The average size of these particles was determined from *Brunauer-Emmet-Teller* (BET) measurements and from transmission electron spectroscopy (TEM) and was found to be *ca.* 5 nm. Due to the high concentration of the particles, agglomeration occurs (see *Fig. 1*). The size distribution of the agglomerates was determined with a scanning mobility particle sizer (SMPS) consisting of a charging device (^{85}Kr-radioactive source), to establish a *Boltzmann* charge distribution on the aerosol, a differential mobility analyzer (DMA; *TSI* model *3071*) for classification, and a condensation particle

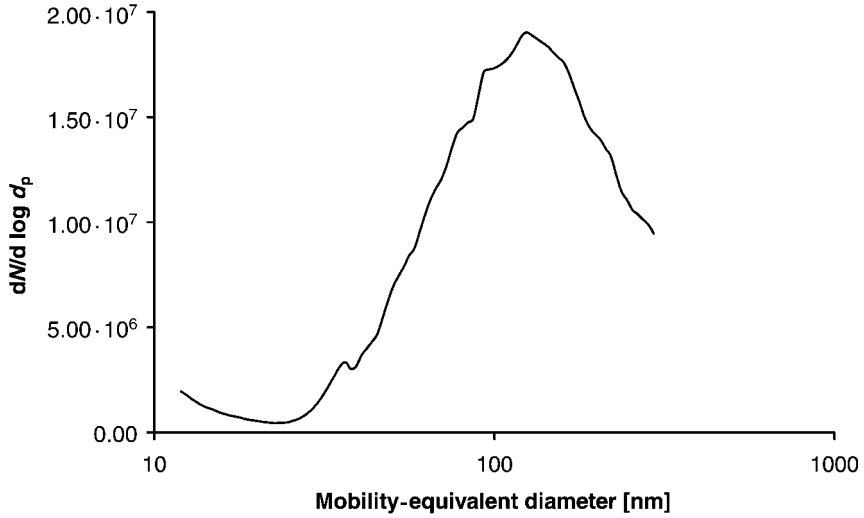

Fig. 4. *Size distribution of the Pt-agglomerates produced in the spark-discharge generator in N_2 as a carrier gas*

counter (CPC; *TSI* model *3022*). The size distribution of the Pt-agglomerates produced in the spark-discharge generator shows a maximum at the (median) mobility diameter of *ca.* 120 nm (*Fig. 4*).

The agglomerates are formed by individual particles (primary particles) held together mostly by *van der Waals* forces [28]. Structures of this kind tend to collapse when treated thermally well below the sintering temperature [29]. The driving force for this structural change is the minimization of the *Gibbs* free energy, the minimum being assigned to the close packed structure [30]. Thermal treatment of the aerosol thus leads to a decrease of the agglomerate diameter and the particle surface accessible for diffusing gas molecules, thereby affecting the catalytic properties of the agglomerate. *Weber* and *Friedlander* [30] assumed kinetics behavior of the rate coefficient of restructuring of an *Arrhenius* form, denoting an exponential dependence on temp., which was verified experimentally with tandem DMA measurements, an experimental technique described in detail by *Schmidt-Ott* [29]. From the rate coefficients for restructuring determined, they found activation energies independent of the number of primary particles in the agglomerate.

To alter the agglomerate structure as a parameter for the catalytic activity, the particles were thermally treated at various temps. The median mobility-equivalent diameter, determined by SMPS measurements, and the specific surface area, determined by BET measurements, are plotted *vs.* the temp. in *Fig. 5*.

The change of the median diameter with the sintering temp. shows only a small change below 400°. For higher temp., the curve drops off rapidly, corresponding to the TEM micrographs showing a structural change at 500° and sintering to massive particles at 700°. The specific surface area reaches a final value of 6 m^2/g at 700° and is thus reduced by approximately a factor of 10 compared to the unsintered agglomerates.

The educt gases H_2 and O_2 are added to the N_2 flow (99.999% N_2) carrying the catalyst particles before entering a variable volume for reaction (*Fig. 6*). All gas flows are controlled *via* mass-flow controllers. For the reaction, H_2 and O_2 were kept at 5 vol-% each. To adsorb O_2 on the particle surface before reaction, the O_2 can be added to the aerosol before the reaction is started, allowing a residence time of *ca.* 5 s sufficient for the coverage of the Pt-surface. The variation of the reaction volume enables us to gather reaction data for several residence times. The water yield from the reaction was low enough to assume constant educt concentrations. Therefore, orders of reaction in respect of H_2 and O_2 had not to be taken into account. For the analysis of the reaction gas, we used an FT-IR spectrometer (*Bruker Vector 22*) equipped with an aerosol flow cell with an optical path length of 225 mm, which was developed and constructed in our institute. The resolution of the spectrometer with respect to water was *ca.* 10 ppm. The low concentration of the aerosol particles did not lead to a measurable shift in the spectra by interactions between IR light and species adsorbed on the particle surface.

Before and after the reaction, the catalyst particles were characterized morphologically by TEM, their size distribution was determined with an SMPS system, and the specific surface could be obtained from BET

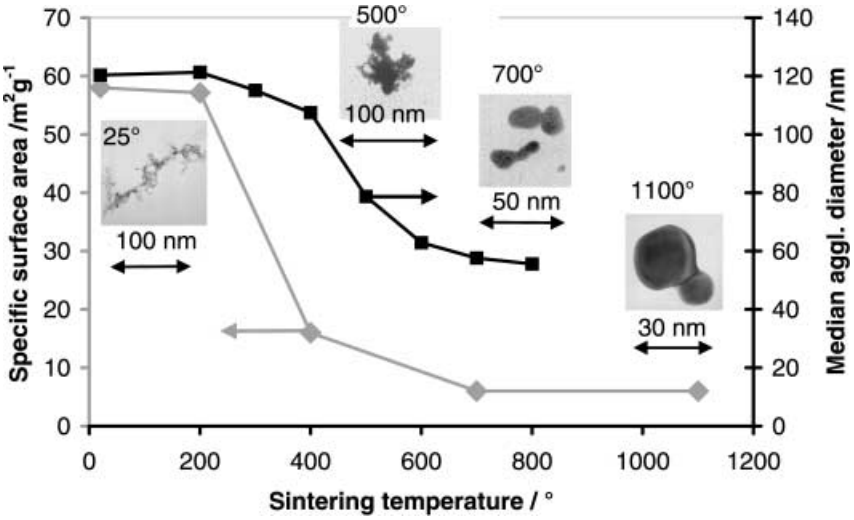

Fig. 5. *Median particle diameter and specific surface area of the agglomerates plotted* vs. *the sintering temperature.* Insets: TEM micrographs of typical particles at 25, 500, 700, and 1100°.

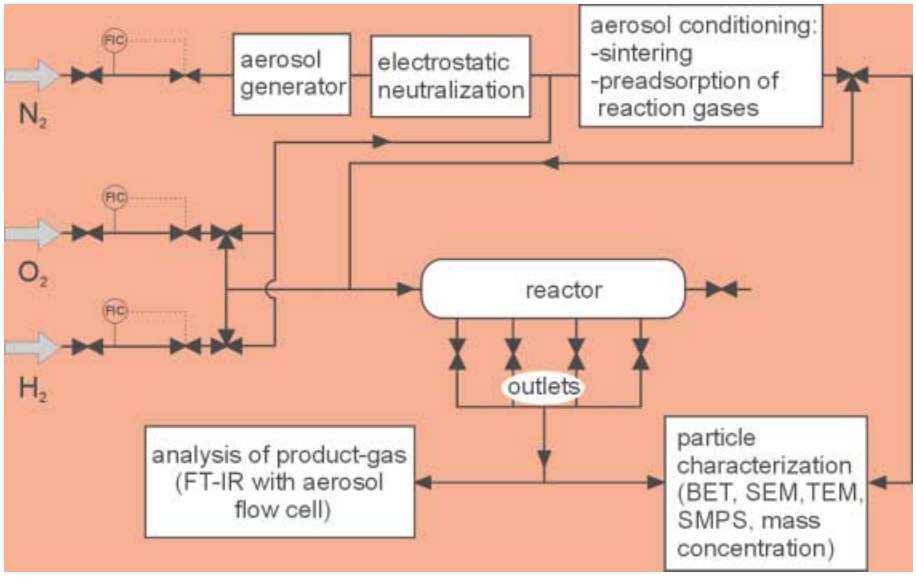

Fig. 6. *Flow chart of the experimental setup for aerosol catalysis*

measurements. With the help of these particle characterization tools, particle properties can be monitored and correlated to the measured catalytic activity.

6. Results and Discussion. – 6.1. *Influence of Initial Surface State.* To study the reaction on a simple geometry, MC simulations as well as experiments were carried out on spheres. The catalytic activity of the particles was expressed as the turn-over rate

(*TOR*), which was defined as the number of molecules produced per surface site and total run time. Experimentally, the *TOR* was determined from the water concentration in the product gas, the total number of surface atoms calculated from the BET surface, and the residence time, which was experimentally determined from pulse measurements. *Fig. 7* shows the results of the MC calculations for various starting conditions. For a surface initially covered with O-atoms, a steep rise of the reaction rate, expressed as the *TOR*, is observed (curve A). This increase in the reaction rate occurs when H-atoms start to adsorb on the surface and the reaction between the adsorbed species begins. The decrease of the *TOR* observed after a culmination point at 0.2 μs results from the decreasing O_{ads} coverage. A kind of poisoning effect of the H_{ads} sets in, blocking surface sites for the adsorption of O-atoms. After approximately 1 s, a plateau of constant *TOR* is reached.

If the surface is initially uncovered, the *TOR* reaches a value initially high, decreasing again when H_{ads} poisoning sets in, leading to a plateau in the *TOR* when equilibrium of the surface species is reached (curve B).

For a surface initially covered with H_{ads}, the *TOR* is already at the level of the plateau of the steady state when the reaction starts. The blockage of surface sites hinders the adsorption of O-atoms (curve C). All the curves, independent of the initial surface state, reach the same final value for the *TOR* when equilibrium is established at steady state.

Conformance between simulation and experiment was observed for the qualitative progression of the curves for the time dependence of the *TOR* for particles precovered

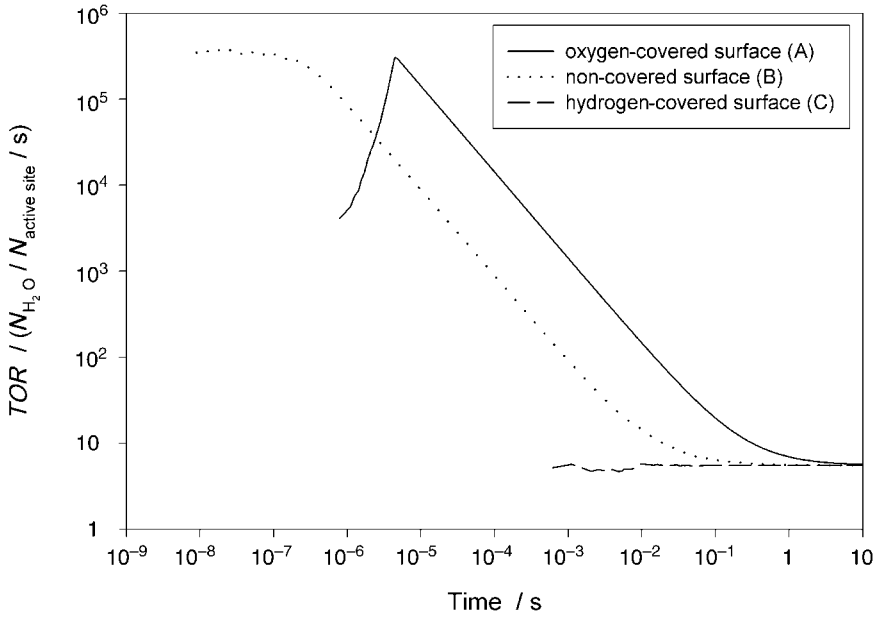

Fig. 7. *MC Simulations for spherical particles initially uncovered with surface species, covered with adsorbed O-atoms, or covered with adsorbed H-atoms before reaction.* N_{H_2O} = number of H_2O molecules produced per surface site ($N_{active\ site}$) and total run time.

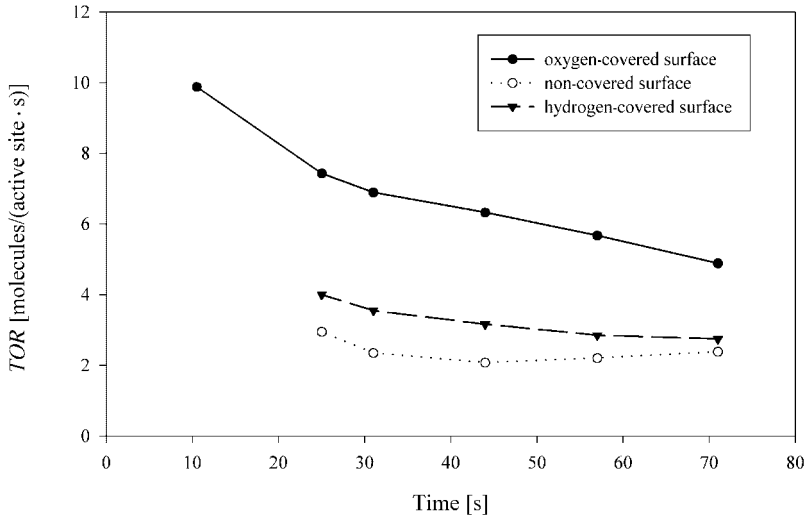

Fig. 8. *Experimentally determined turn-over rates* (TOR) *for Pt-agglomerates for varied initial surface states: uncovered, covered with adsorbed O-atoms, or covered with adsorbed H-atoms before reaction*

with O-atoms and for those uncovered initially (*Fig. 8*). Due to the extensive demand for machine time, the MC simulation could so far not be carried out for uncovered agglomerates and for those precovered with H-atoms. For a qualitative discussion we, therefore, refer to the results obtained from the simulation of the spheres. An increase in the initial rate due to the participation of the inner surface area occurred when O-atoms were adsorbed previously, as observed for the MC simulation. The effect of H-poisoning is also present, as can be seen by the less-pronounced but still distinct decrease of the *TOR* with time for the initially uncovered agglomerates. The curves representing the experiments carried out with the pre-adsorption of H-atoms on the surface, though, show increased *TOR* with respect to the uncovered particles, thus deviating from the results of the simulation. A possible reason for this is a cleaning effect brought about by a reduction of adsorbed species on the Pt-surface.

When steady state is reached, the three curves approach each other again, and the initial surface state loses its influence on the catalytic reaction. In this respect, agreement between model and simulation is obtained.

6.2. *Fraction of Exposed Surface.* The variation of the ratio of outer surface to the total surface area was carried out both in the MC simulation and experimentally. For the MC simulation, the results are plotted in *Fig. 9*. The *TOR* for the sphere was already discussed above. For an agglomerate with a value for K of 0.749, representing a rather open agglomerate, the initial peak of the *TOR* is less distinct and becomes even broader for an agglomerate with a K value of 0.305, representing a rather compact structure. The peak broadening is due to the reaction of the O-atoms adsorbed on the inner surface of the agglomerate with H-atoms accessing by surface diffusion. After the internal O-atoms have reacted, the significance of the inner surface for the reaction vanishes since the slow-diffusing O-atoms (compared to the H-atoms) are unable to reach it and react shortly after adsorption from the gas phase to the outer surface of the

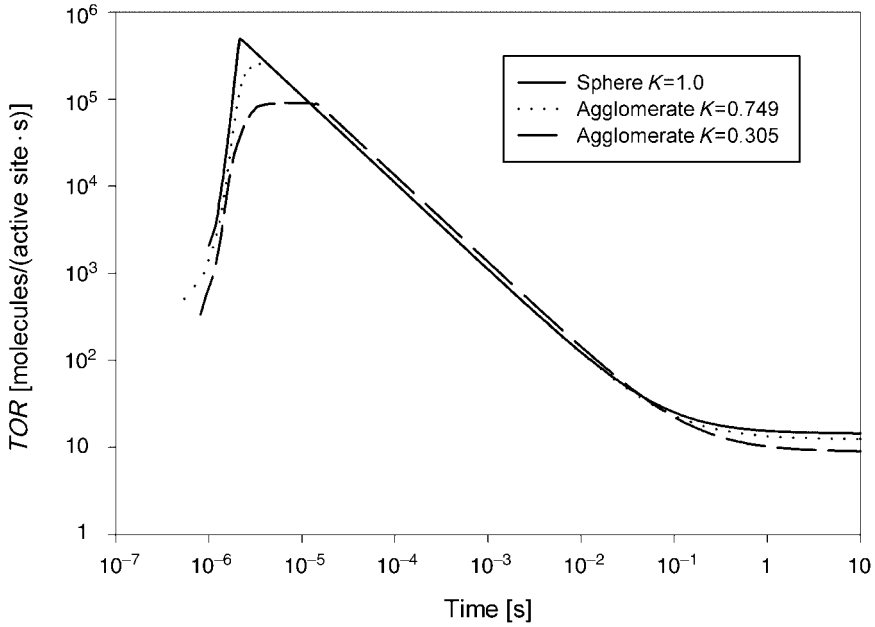

Fig. 9. *Turn-over rates* (*TOR*) *determined for different fractions of exposed surface* K *of the model agglomerate for the MC simulation.* The particle surface was uncovered initially. $K = 1$, sphere; low values of K represent compact agglomerates.

agglomerate. Consequently, H-poisoning on the outer surface sets in, reducing the *TOR* until steady state is reached. The values of the *TOR* for steady state show an increasing tendency for rising values of K. Since the *TOR* is based on the total number of surface sites in the lattice, the values calculated are lowered when the surface available for the reaction is smaller than the total surface. Thus, an increase in internal surface, which does not contribute to the reaction at steady state, leads to a decrease in the *TOR*. Since the MC simulation is based on the assumption that all surface sites are equally active and that the surfaces of the agglomerate and the sphere are assembled of the same sites, these results are plausible.

The variation in the function of outer surface of the agglomerates by sintering experiments showed a close dependence of the *TOR* at steady state (residence time: 57 s) on the median agglomerate diameter, which represents a measure of the outer surface of the agglomerate (*Fig. 10*). This result illustrates the importance of the outer surface for the reaction and corresponds to the *TOR* determined from the MC simulation for steady state, which is also closely related to the amount of outer surface.

6.3. *Rate Enhancement for Nanoparticle Agglomerates.* The steady-state values of the *TOR* were determined experimentally and from the MC simulation for the agglomerates and the solid spheres. The *Table* shows the ratios of the determined values calculated on the basis of the total surface area, BET for the experimental surface sites for the simulation, and on the basis of the external surface determined being represented by the mobility-equivalent sphere experimentally and the surface sites

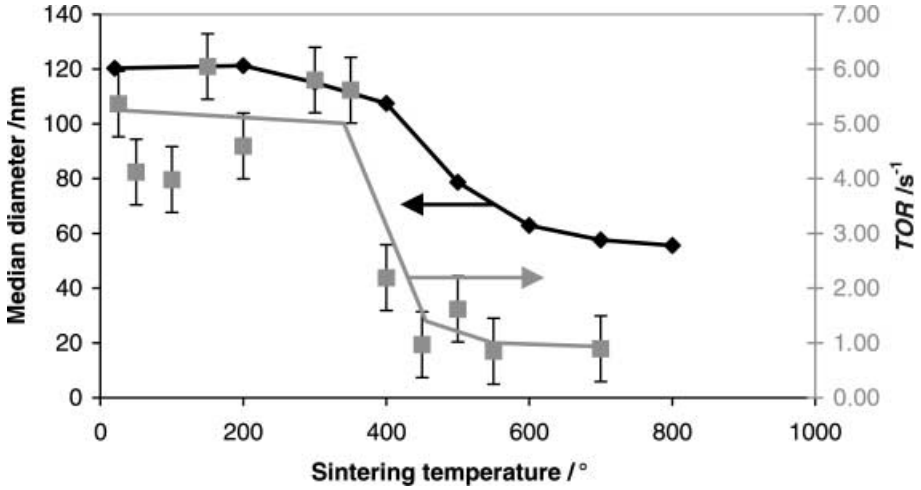

Fig. 10. *Dependence of turn-over rates* (*TOR*) *and median diameter of the Pt-agglomerates on the sintering temperature of the thermal pre-treatment of the particles*

assigned to the white area in *Fig. 2*. The results for the simulation show a close dependence of the steady-state *TOR* on the fraction of external surface. The value for the ratio of *TOR* calculated for the total surface was 0.53, closely matching the value of *K*, which was 0.55 for the simulation. The ratio of *TOR* for agglomerates and spheres based on the external surface area was found to be 0.96, which signifies that, within error, the catalytic activity of the agglomerates solely depends on the external surface at steady state for the MC simulation.

Table 1. *Ratios of* TOR *for Agglomerates and Spheres Calculated from the MC Model and the Experiments Based on the Total Surface Area of the Agglomerates and the External Surface Area*

	MC model: TOR_{aggl}/TOR_{sphere}	Experiment: TOR_{aggl}/TOR_{sphere}
Calculated for the total surface	0.53	2.6
Calculated for the external surface	0.96	5.75

A different picture is given by the results from the experimental studies. There, the *TOR* of the agglomerates is higher than that of spherical particles, even when related to the total surface area. This enhancement becomes even more pronounced when relating the *TOR* to the exposed surface (*Table*). The origin of this enhancement is yet unclear. There are several hypotheses to be confirmed or ruled out by further experiments. During tempering, the agglomerate structure changes in many ways. First the particle surface state may change, then the interparticle contact can be altered, and finally the primary particle size increases, as can be deduced from the specific surface area shown in *Fig. 5*. An explanation for the mentioned effect could be an enhanced catalytic activity of the 5-nm primary particles in the unsintered agglomerate to the sintered 50-nm particles. This hypothesis is supported by the work of *Bowker et al.*, who observed a dependence of the reactivity for the dissociation of O_2 from Pd on the

curvature of the particle surface and found a strongly enhanced reaction rate at the tips of elongated nanoparticles [1].

6.4. *Sticking Probability.* Another deviation of the experimental data from the MC simulation is the temporal behavior of the catalytic reaction. The time until steady state is established in the experiments ranges from 45 s to approximately 80 s, whereas in the MC simulation (carried out with a bulk value for the sticking probability of H_2) steady state was established after times shorter than 1 s.

The time scale relevant for the catalytic combustion of H_2 on Pt, as simulated with our MC model, is strongly dependent on the sticking probabilities of the H- and O-atoms on the catalyst surface, since the attachment of the educt molecules to the surface is rate-determining. For the simulations, the initial intrinsic sticking probability of H-atoms was assumed to be 0.2, averaged over values found for H-atoms on polycrystalline bulk Pt-surfaces, the initial sticking probability of O-atoms was assumed to be 0.28. For gas-borne nanoparticles, though, *Müller et al.* experimentally found values lowered by a factor of *ca.* 500 for the sticking probability of O-atoms on Ni-nanoparticles [31]. *Fig. 11* shows the dependence of the temporal behavior of the reaction on the variation of the sticking probability. The kinetics of the *TOR* calculated with the reduced sticking probabilities with a constant ratio between the values for H- and O-atoms, leads to a distinctive shift of the time scale compared to the calculations carried out with the bulk value for polycrystalline Pt. The reduced sticking probability can thus in part explain the deviation in the time scales for simulation and experiment.

Calculations of *TOR* for a varied ratio of the sticking probability of H-atoms to the one of O-atoms on spherical particles showed that a relative increase of the sticking

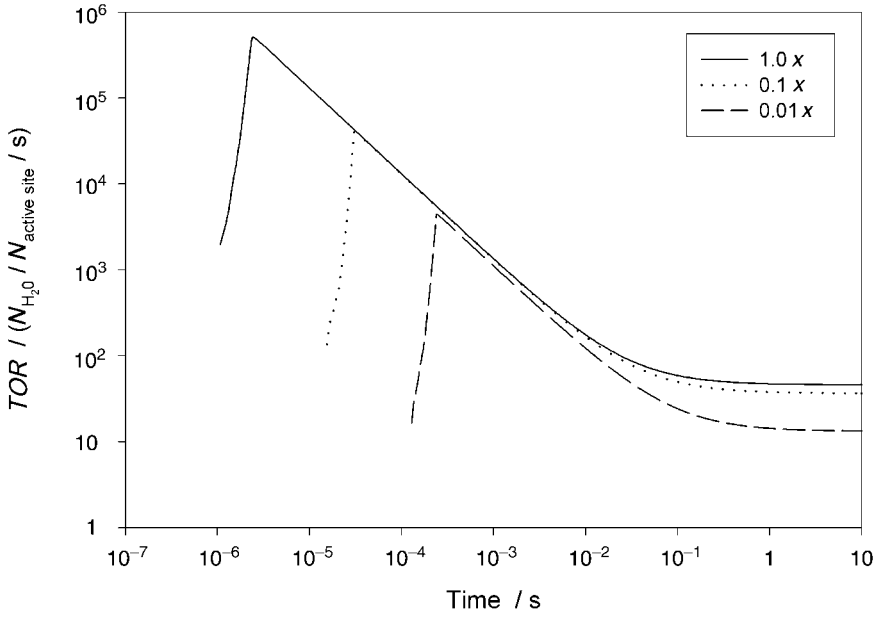

Fig. 11. *Variation of the sticking probabilities of H- and O-atoms on the surface of spherical Pt-particles.* $x =$ Value for polycrystalline Pt.

probability of O-atoms on the Pt-surface (as indicated by *Bowker et al.* [1]) also leads to a shift in the time scale towards higher values. Taking into account a time delay caused by a noninstantaneous reaction between the educt surface species would also alter the temporal behavior to better meet the experimental results.

On the basis of the currently available data, a definitive conclusion about the mechanism responsible for the observed time shift in reaction kinetics cannot be drawn. This issue has to be clarified by future simulation and experimental work.

7. Conclusions. – The temporal evolution of the *TOR* was determined both with the MC simulation and experimentally. The trends of both curves are similar, showing a drastic decrease at short reaction times. The time scales though deviate strongly. This discrepancy between MC simulation and experiment may be explained by a lowered sticking probability on nanoparticles compared to bulk surfaces as well as a relatively higher sticking probability for O-atoms compared to H-atoms.

The experimentally determined *TOR* based on the total surface for agglomerates of 5-nm Pt-particles revealed a remarkably higher catalytic activity than the 50-nm spheres. The origin of this enhancement is yet uncertain. The restructuring processes, which lead to the transformation of the agglomerate to the solid sphere, cause a substantial change at the particle surface. The increase of the particle size leads to a decrease in surface curvature, which leads to a change in dissociation kinetics of O_2 [1].

The catalytic activity showed a strong dependence on the fraction of exposed surface of the agglomerates for both the simulation and the experiment. This illustrates the importance of the accessability of the catalyst surface for direct impingement by gas molecules.

The partial funding of this work by the *DFG* is gratefully acknowledged.

REFERENCES

[1] M. Bowker, R. Smith, R. A. Bennett, *Surf. Sci.* **2001**, *478*, L309.
[2] L. Piccolo, R. C. Henry, *Appl. Surf. Sci.* **2000**, *162/163*, 670.
[3] M. A. Glikin, *Theor. Found. Chem. Engl*. **1996**, *30*, 390.
[4] A. P. Weber, M. Seipenbusch, C. Thanner, G. Kasper, *J. Nanoparticle Res.* **1999**, *1*, 253.
[5] G. B. Fisher, J. L. Gland, S. J. Schmieg, *J. Vac. Sci. Technol.* **1982**, *20*, 518.
[6] A. Schmidt-Ott, U. Baltensperger, H. W. Gäggeler, D. T. Jost, *J. Aerosol Sci.* **1990**, *21*, 711.
[7] H. Ikeda, J. Sato, F. A. Williams, *Surf. Sci.* **1995**, *326*, 11.
[8] O. Deutschmann, Ph. D. Thesis, Ruprecht-Karls-Universität, Heidelberg, 1996.
[9] V. P. Zhdanov, B. Kasemo, *Surf. Sci. Rep.* **2000**, *39*, 25.
[10] K. Christmann, 'Electrocatalysis', Wiley-VCH, Weinheim, 1998, p. 1.
[11] B. Poelsema, L. K. Verheij, G. Comsa, *Surf. Sci.* **1985**, *152/153*, 496.
[12] B. Hellsing, B. Kasemo, S. Ljungström, A. Rosén, T. Wahnström, *Surf. Sci.* **1987**, *189/190*, 851.
[13] P. J. Kisliuk, *J. Chem. Phys. Solids* **1957**, *3*, 95.
[14] R. Meier, Ph. D. Thesis, Freie Universität Berlin, Berlin, 1999.
[15] K. Christmann, G. Ertl, T. Pignet, *Surf. Sci.* **1976**, *54*, 365.
[16] S. Völkening, K. Bedürftig, K. Jacobi, J. Wintterlin, G. Ertl, *Phys. Rev. Lett.* **1999**, *83*, 2672.
[17] J. L. Gland, B. A. Sexton, G. B. Fisher, *Surf. Sci.* **1980**, *95*, 587.
[18] B. Hellsing, B. Kasemo, V. P. Zhdanov, *J. Catal.* **1991**, *132*, 210.
[19] L. K. Verheij, M. B. Hugenschmidt, *Surf. Sci.* **1998**, *416*, 37.
[20] G. T. Fujimoto, G. S. Selwyn, J. T. Keiser, M. C. Lin, *J. Phys. Chem.* **1983**, *87*, 1906.
[21] A. P. Graham, A. Menzel, J. P. Toennies, *J. Chem. Phys.* **1999**, *111*, 1676.

[22] J. Wintterlin, R. Schuster, G. Ertl, *Phys. Rev. Lett.* **1996**, *77*, 123.
[23] J. L. Gland, G. Fisher, E. B. Kollin, *J. Catal.* **1982**, *77*, 263.
[24] S. Völkening (*Bayer AG*, Leverkusen), personal communication.
[25] K. L. Johnson, K. Kendall, A. D. Roberts, *Proc. R. Soc. Lond., A* **1971**, *324*, 301.
[26] A. P. Weber, S. K. Friedlander, *J. Aerosol Sci.* **1997**, *28*, Suppl. 1, S765.
[27] S. Schwyn, J. L. Garwin, A. Schmidt-Ott, *J. Aerosol Sci.* **1988**, *19*, 639.
[28] A. Schmidt-Ott, H. Burtscher, *J. Colloid Interface Sci.* **1982**, *89*, 353.
[29] A. Schmidt-Ott, *J. Aerosol Sci.* **1988**, *19*, 553.
[30] A. P. Weber, S. K. Friedlander, *J. Aerosol Sci.* **1997**, *28*, 179.
[31] U. Müller, M. Ammann, H. Burtscher, A. Schmidt-Ott, *Phys. Rev. B* **1991**, *44*, 8284.

Received June 6, 2001